Adsorption and Reaction of Methanol on Stoichiometric and Defective $SrTiO_3$(100) Surfaces

Li-Qiong Wang,*,† Kim F. Ferris,† Samina Azad,‡ and Mark H. Engelhard‡

Material Science Division and Environmental Molecular Science Laboratories, Pacific Northwest National Laboratory, Richland, Washington 99354

Received: April 15, 2004; In Final Form: September 24, 2004

The adsorption and reaction of methanol (CH_3OH) on stoichiometric (TiO_2-terminated) and reduced $SrTiO_3$(100) surfaces have been investigated using temperature-programmed desorption (TPD), X-ray photoelectron spectroscopy (XPS), and first-principles density-functional calculations. Methanol adsorbs mostly nondissociatively on the stoichiometric $SrTiO_3$(100) surface that contains predominately Ti^{4+} cations. Desorption of a monolayer methanol from the stoichiometric surface is observed at ~250 K, whereas desorption of a multilayer methanol is found to occur at ~140 K. Theoretical calculations predict weak adsorption of methanol on TiO_2-terminated $SrTiO_3$(100) surfaces, in agreement with the experimental results. However, the reduced $SrTiO_3$(100) surface containing Ti^{3+} cations exhibits higher reactivity toward adsorbed methanol, and H_2, CH_4, and CO are the major decomposition products. The surface defects on the reduced $SrTiO_3$(100) surface are partially reoxidized upon saturation exposure of CH_3OH onto this surface at 300 K.

1. Introduction

Surface chemistry of metal oxides plays an important role in modern technology, particularly in the development of catalysts, gas sensors, fuel cells, and semiconductor devices. The adsorption of small molecules onto metal oxide surfaces is often used for probing the physical and chemical properties of metal oxides. The reactivity of oxide surfaces is largely influenced by the presence of surface defects, the acid−base properties of adsorbed molecules and the oxide surface, and the geometric arrangement of the surface atoms. Both TiO_2 and $SrTiO_3$ single crystals have been widely used as model surfaces to study structural and chemical properties of oxide surfaces because of their availability as well as the varieties of oxidation states and coordination environments they provide. Oxygen vacancies or other more complex surface defects associated with the reduced states of these surfaces are known to promote the reactions of adsorbed molecules. The defect sites on the reduced $SrTiO_3$(100) surfaces are reoxidized by extraction of the oxygen atoms from adsorbed molecules.[1] The ionic nature of metal oxides leads to a predominance of acid−base interactions where metal cations and oxygen anions are acid and basic sites, respectively, and their reactivity is often described in terms of acid−base properties of particular sites in relation to their geometric arrangement.

Interactions of methanol on single-crystal TiO_2 surfaces have been studied previously under ultrahigh-vacuum condition.[2−9] Onishi et al. have reported that methanol adsorbs molecularly on the (110) and stepped (441) TiO_2 surfaces at 300 K,[3] whereas on oxidized TiO_2(110)[2] and -(001)[7,8] as well as on reduced TiO_2-(110)[5] and TiO_2(001)[8] surfaces it is found to adsorb dissociatively. Both molecular methanol and methoxy species were observed on a highly reduced (Ar^+-bombarded) TiO_2(001) surface upon exposure to CH_3OH at 300 K, but only methoxy species were present on the (011)- and (114)-faceted TiO_2(001) surfaces at 300 K.[8] The coordination-unsaturated Ti cations and adjacent oxygen vacancies lead to the dissociative adsorption of methanol on these surfaces. The interaction between the adsorbed methoxy species and the two different binding sites on TiO_2(110) surfaces[2] results in a variety of reaction products: the majority of the methoxy species bound to a Ti^{4+} cation recombine at low temperature with bridging hydroxyl groups and desorb as methanol, whereas the methoxy species adsorbed on anion vacancy sites desorb as methane at higher temperatures. A small fraction of defects created by electron beam exposure and Ar^+ bombardment on (110) and (100) TiO_2 surfaces is found to be healed upon saturation exposure to methanol.[4]

$SrTiO_3$ surfaces have attracted considerable attention due to their photocatalytic properties and their important role in the photoelectrolysis of water under illumination with band-gap radiation even in the absence of an applied bias.[10] Although, as noted above, the reactions of methanol have been investigated extensively on TiO_2 surfaces, only one study thus far has reported the reductive coupling desorption for methanol on a reduced $SrTiO_3$(110) surface.[11] To our knowledge, no temperature-programmed desorption (TPD) studies of methanol on $SrTiO_3$(100) surfaces have been reported.

This study focuses on the interaction of methanol with the TiO_2-terminated stoichiometric (or fully oxidized) and defective (or reduced) $SrTiO_3$(100) surfaces. $SrTiO_3$(100) surfaces have two possible nonpolar surface terminations: a SrO-terminated surface and a TiO_2-terminated surface. The TiO_2-terminated stoichiometric $SrTiO_3$(100), schematically illustrated in Figure 1, displays a different geometric arrangement of surface Ti and O atoms as compared with TiO_2(110) and -(100) surfaces. Instead of rows of two-coordinate bridging oxygen atoms lying above rows of Ti atoms as in the cases of TiO_2(110) and -(100) surfaces, the cations on the TiO_2-terminated $SrTiO_3$(100) surface lie essentially on the same plane as the oxygen atoms. Thus, by studying the TiO_2-terminated $SrTiO_3$(100) surfaces, we can examine the influence of Ti and O atomic arrangements and the bonding configurations on this surface, as well as the effect

* To whom correspondence should be addressed. E-mail: lq.wang@pnl.gov.
† Material Science Division.
‡ Environmental Molecular Science Laboratories.

10.1021/jp048338t CCC: $30.25
Published on Web 02/11/2005

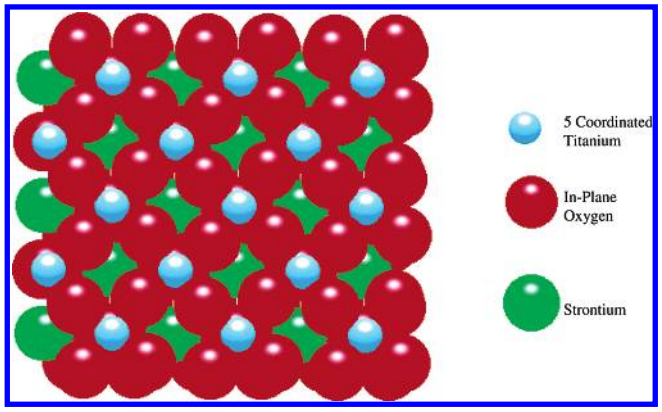

Figure 1. Schematic model for the TiO_2-terminated $SrTiO_3$(100) surface.

of the bridging oxygen atoms on the adsorption and reaction of methanol.

A variety of theoretical models have been used to investigate the nature of bound water and methanol on the TiO_2 surfaces.[12−15] Electronic structure calculations for water and methanol adsorbed onto the fully oxidized (110) and (100) rutile TiO_2 surfaces indicate that the dissociative form is thermodynamically favored in each case; however, there is a potential energy barrier for water dissociation on the (110) surface and methanol on both surfaces.[12] Thus far, no theoretical calculations have been reported for the adsorption of methanol and water on the $SrTiO_3$-(100) surface using first-principle density function calculations. This study also presents first-principles density-functional calculations on interactions of methanol and water on the stoichiometric $SrTiO_3$(100) surfaces.

2. Experimental Section

TPD experiments were carried out in a ultrahigh-vacuum chamber at a base pressure of $\sim 2 \times 10^{-10}$ Torr. The chamber was equipped with a single-pass cylindrical mirror analyzer for Auger electron spectroscopy (AES), a quadrupole mass spectrometer for TPD, optics for low-energy electron diffraction (LEED), and an ion gun for sample cleaning. TPD data were collected using a heating rate of ~1 K/s, and desorbing species were detected using a UTI quadrupole mass spectrometer interfaced to a PC, allowing nine masses to be monitored sequentially during the desorption sweep. The sample was dosed via back-filling of the chamber with reactant gases, and pressures were not corrected for ionization gauge sensitivities.

The XPS experiments were carried out in a second UHV chamber at a base pressure of $\sim 5 \times 10^{-10}$ Torr. X-ray photoelectron spectroscopy (XPS) measurements were made on a Physical-Electronics Quantum 2000 scanning ESCA microprobe system that uses a hemispherical analyzer. Monochromatic Al Kα X-rays (1486.7) with X-ray spot size of 1.5 mm × 0.2 mm were used to generate the spectra. The multiplex data were collected with a pass energy of 23.5 eV. The collected data were referenced to an energy scale with binding energies for Au 4f at 84 ± 0.03 eV and Cu 2p 3/2 at 932.67 ± 0.03 eV.

The $SrTiO_3$(100) crystal (10 × 10 × 2) was purchased from Princeton Scientific and was epi-polished on both sides and cut with 0.5 mm×2.0 mm slots around the four sides of the crystal. The crystal was mounted on a polished tantalum plate with a 0.025 mm thick gold foil sandwiched between the two surfaces. Chromel−alumel thermocouple wires were glued to the sample using a ceramic glue. The sample can be resistively heated to 1000 K, and cooled to 120 K by thermal contact with a liquid nitrogen filled reservoir. The samples were cleaned by Ar^+ sputtering. The stoichiometric surfaces were obtained by annealing sputtered surfaces at 800−850 K for 10 min, in 1×10^{-7} Torr O_2. The reduced surfaces for TPD measurements were prepared by Ar^+ bombardment at 1 keV for 20 min. Cleanliness of the surfaces was verified by AES measurements prior to the TPD and XPS experiments.

Methanol (CH_3OH, ACS HPLC grade, 99.9% purity) was obtained from Aldrich. Several freeze−pump−thaw cycles with liquid nitrogen were performed on methanol prior to the experiments. Methanol was dosed onto the crystal, which was held at ~120 K, through a leak valve into the main chamber at various low exposures for TPD measurements. The TPD system was not calibrated to measure the exact coverage, and the 1 langmuir exposure reported here may not be equivalent to the 1 monolayer methanol coverage (or the number density of Ti^{4+} sites of 6.55×10^{14} atoms/cm^2).

3. Computational Methods

First-principles DFT computations have been performed using the Cerius2 program system.[16] Structural energies as well as equilibrium unit cell and atomic geometries were obtained from force optimization methods using generalized gradient-corrected (GGA) forms of the local density approximation[17] and ultrasoft pseudopotentials.[18] Bulk and slab structural parameters were determined using the CASTEP electronic structure program utilizing a plane wave basis set with a 380 eV cutoff energy.[19] Initial starting structures were taken from experimental determinations. To investigate the localized adsorption reaction and the associated charge redistributions, DMOL3 computations were performed using numerical basis sets of double-ζ plus polarization function quality to describe the valence orbitals and pseudopotentials for the core regions. These latter computations have been performed with the GGA nonlocal exchange-correlation functional. Charge distributions were estimated using the Hirshfeld charge partitioning formalism.[20] Recent results using this methodology have shown excellent agreement for the structure and adsorption characteristics of metal oxide systems.[21−23]

4. Results and Discussion

4.1. Interaction of Methanol with Stoichiometric $SrTiO_3$-(100) Surfaces. Various reconstructions on SrTiO3(100) surfaces have been observed previously, depending on the sample preparation conditions.[24−31] Fully oxidized $SrTiO_3$(100) surfaces, prepared in our studies by sputtering followed by annealing at 800−850 K in O_2 show a 1 × 1 LEED pattern. Previous ion scattering studies[32,33] have shown that similarly prepared $SrTiO_3$-(100) single-crystal surfaces were predominantly terminated by TiO_2 atomic planes. Thus, the stoichiometric or fully oxidized $SrTiO_3$(100) surfaces used in our studies should be mostly (1 × 1) TiO_2-terminated. Figure 2 displays a series of 31 amu TPD spectra monitoring desorption of CH_3OH, following adsorption of 0.1 (a), 0.5 (b), 1 (c), 2 (d), and 4 langmuirs (e) of CH_3OH on the stoichiometric $SrTiO_3$(100) surface at 120 K. Spectrum 2a consists of a single feature centered at ~310 K for desorption of 0.1 langmuir of methanol from this surface. This desorption feature grows in intensity and shifts gradually to lower temperatures with increasing exposure of methanol on this surface. The 310 K feature shifts to 280 K for 0.5 langmuir of methanol (spectrum 2b) and to 260 K for 1 langmuir of methanol (spectrum 2c) on the same surface. A smaller feature appears at ~160 K for adsorption of 1 langmuir of methanol on this surface, and this feature shifts to 140 K when the methanol exposure is increased to 4 langmuirs (spectra 2d,e).

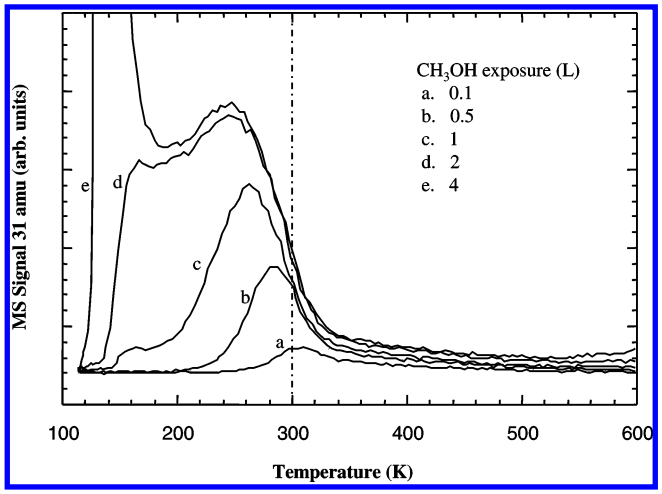

Figure 2. TPD spectra of 31 amu for CH_3OH adsorbed onto a stoichiometric TiO_2-terminated $SrTiO_3$(100) surface at 120 K following adsorption of 0.1 (a), 0.5 (b), 1 (c), 2 (d), and 4 langmuirs of CH_3OH (e).

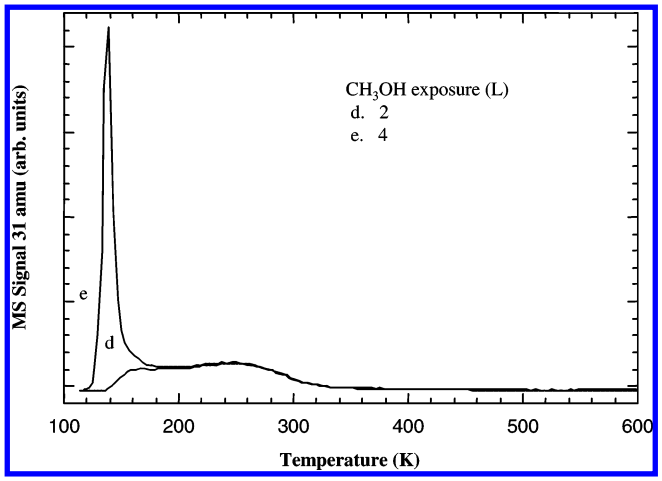

Figure 3. TPD spectra of 31 amu for CH_3OH adsorbed onto a stoichiometric TiO_2-terminated $SrTiO_3$(100) surface at 120 K. Spectra "d" and "e" (also shown in Figure 2) correspond to 2 and 4 langmuirs of CH_3OH, respectively.

Desorption of water from metal oxide surfaces at temperatures higher than 300 K is known to result from dissociative adsorption of water and recombination of adsorbed OH species.[34] Previous TPD studies[35,36] of H_2O on TiO_2(110) and TiO_2-(100) surfaces assign the resolved water TPD features at temperatures above 300 K to a dissociative state of water, whereas the features at temperatures below 300 K have been attributed to a nondissociative state of water. These assumptions agree well with high-resolution energy loss spectroscopy (HREELS) and TPD studies on ^{18}O-enriched surfaces.[36,37] Since the majority of methanol desorb from the stoichiometric $SrTiO_3$-(100) at temperatures below 300 K and water and methanol show similar acid−base properties, we assume that methanol adsorbs mostly nondissociatively on this surface. The broad TPD feature that shifts from 310 to 260 K in Figure 2 can be assigned to the molecular desorption of chemisorbed methanol on Ti^{4+} sites. The large shift in temperature of this feature with increasing coverage is presumably due to the repulsive interactions between the adsorbed methanol molecules.

Figure 3 compares 31 amu TPD spectra for adsorption of 2 and 4 langmuirs of methanol on a fully oxidized $SrTiO_3$(100). A full-scale 31 amu TPD plot for adsorption of 4 langmuirs of methanol on the oxidized surface is given in Figure 3, where a large narrow peak appears at 140 K and the leading edge of the TPD spectra is not coincident to increasing methanol exposure. Similar TPD spectra have been observed in our previous water TPD study.[38] It was found that the formation of an intermediate water layer is required to bring the hexagonal multilayer ice into registry with the mostly square monolayer structure adsorbed directly on the oxide surface.[39] The noncoincident leading edge in TPD spectra of water on $SrTiO_3$(100) surfaces is the result of the structural difference between the second layer and thicker layers of water. On the basis of the previous water study,[38] we assign the relatively broad desorption feature at ∼180 K in Figure 2d,e to the desorption of weakly bound methanol in the intermediate or the second layer of methanol, whereas we attribute a large narrow peak at 140 K in Figure 3e to the multilayer methanol desorption.

There is a significant difference in TPD spectra obtained for desorption of methanol on a vacuum-annealed TiO_2(110) (5−10% oxygen vacancies)[5] and on a stoichiometric $SrTiO_3$(100) surface. Upon monolayer coverage, more than a half-monolayer of methanol desorbs from a TiO_2(110) surface at temperatures above 300 K with the desorption peak centered at 295 K. The 295 K state is assigned to the molecular adsorption on the Ti^{4+} sites on a fully oxidized surface. However, only a small percentage of methanol desorbs from a stoichiometric $SrTiO_3$-(100) surface at temperatures above 300 K with the molecular desorption peak centered at 240 K, indicating that methanol binds more strongly to TiO_2(110) than to $SrTiO_3$(100) surfaces. The nature of the Ti^{4+} cation sites is found to be more covalent on the TiO_2-terminated $SrTiO_3$(100) compared to the same sites on the TiO_2 surfaces on the basis of electronic structural calculations,[40,41] and these differences can be attributed primarily to the influence of the Sr cations on the electronic structure of the Ti cations in the mixed oxide of $SrTiO_3$. In particular as was proposed in previous calculations on the energetic of mixed metal oxide surfaces, in the mixing of two oxides (one having a more ionic cation than the other), the ionic properties of the more ionic cation are expected to increase further, while the covalent properties of the more covalent ion should also be enhanced. Since Sr is a more ionic cation than Ti, Sr is more ionic in $SrTiO_3$ than in SrO and Ti in $SrTiO_3$ is more covalent than in TiO_2. Thus, either the higher covalence or weaker acidity of Ti^{4+} cations on $SrTiO_3$(100) surfaces results in a weaker acid−base interaction between Ti^{4+} sites and methanol. The absence of the bridging oxygen atoms on the $SrTiO_3$(100) surface that strengthens the binding of methanol via hydrogen bonding is most likely to be partially responsible for the weaker adsorption of methanol on $SrTiO_3$(100). Thus, it is reasonable that TiO_2-terminated $SrTiO_3$(100) exhibits a weaker interaction with methanol compared to similar interactions on the TiO_2-(110) surfaces. On the basis of a simple Redhead analysis,[42] assuming preexponential factor of 1×10^{13} s^{-1}, we estimate a first-order desorption activation energy of ∼15 kcal/mol for desorption of methanol (240 K feature) from the stoichiometric $SrTiO_3$(100) following adsorption at 120 K. Using the same Redhead analysis, a larger desorption activation energy of ∼18 kcal/mol is obtained for desorption of methanol (295 K feature) from the TiO_2(110) surface, further indicating that methanol binds stronger on TiO_2(110) than on $SrTiO_3$(110) surfaces.

As compared with the desorption of methanol from stoichiometric $SrTiO_3$(100) surfaces (a desorption activation energy of ∼15 kcal/mol), desorption of water from the same surface occurs at lower temperature, 200 K, corresponding to a lower desorption activation energy of ∼12.5 kcal/mol using the Redhead analysis.[38] In addition, the first principles electronic structure

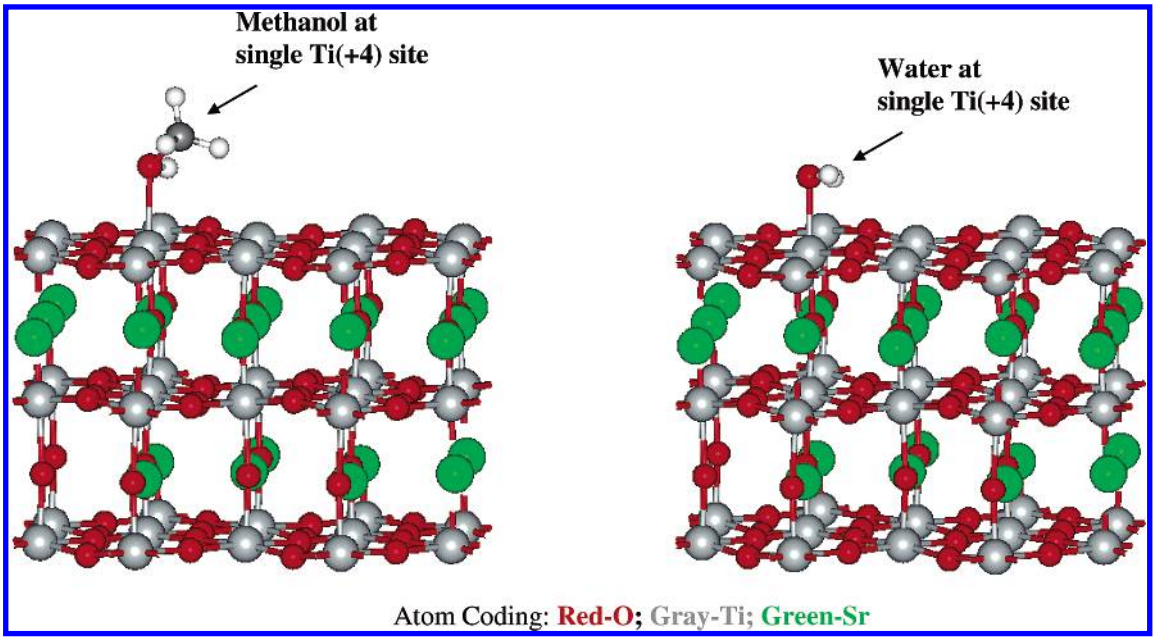

Figure 4. Schematic illustrations of the adsorption geometries for methanol and water on TiO_2-terminated $SrTiO_3$(100) surfaces.

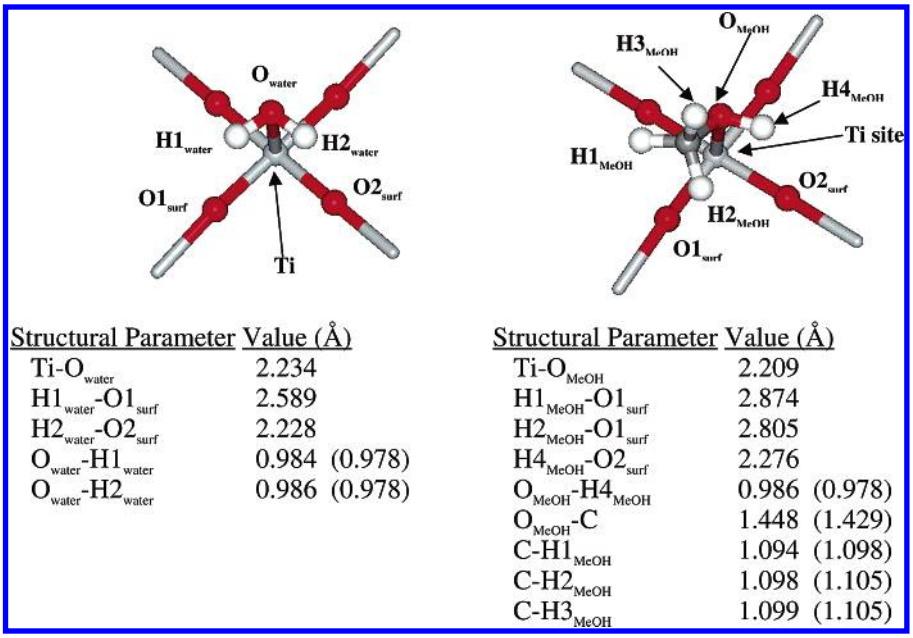

Structural Parameter	Value (Å)	
Ti-O_{water}	2.234	
$H1_{water}$-$O1_{surf}$	2.589	
$H2_{water}$-$O2_{surf}$	2.228	
O_{water}-$H1_{water}$	0.984	(0.978)
O_{water}-$H2_{water}$	0.986	(0.978)

Structural Parameter	Value (Å)	
Ti-O_{MeOH}	2.209	
$H1_{MeOH}$-$O1_{surf}$	2.874	
$H2_{MeOH}$-$O1_{surf}$	2.805	
$H4_{MeOH}$-$O2_{surf}$	2.276	
O_{MeOH}-$H4_{MeOH}$	0.986	(0.978)
O_{MeOH}-C	1.448	(1.429)
C-$H1_{MeOH}$	1.094	(1.098)
C-$H2_{MeOH}$	1.098	(1.105)
C-$H3_{MeOH}$	1.099	(1.105)

Figure 5. Structural parameters for water and methanol adsorption onto the $SrTiO_3$ surface as determined by first-principles calculation using the DZP (double-ζ plus polarization) basis set. The view of the adsorption site is taken from above the surface and omits second layer containing Sr ions for visual clarity. Values in parentheses are for free molecule without surface adsorption interaction. Atom coding: red, O; gray, Ti; white, H.

calculations, performed in this study, give binding energies of 19.4 and 19.1 kcal/mol for methanol and water on stoichiometric $SrTiO_3$(100) surfaces, respectively. On the basis of these results, the interaction of water with $SrTiO_3$(100) is marginally weaker than that of methanol with the same surface.

Schematic adsorption geometries for methanol and water on TiO_2-terminated $SrTiO_3$(100) surfaces are illustrated in Figure 4. The structural parameters as determined by first-principles calculations are given in Figure 5. Water adsorbs on the $SrTiO_3$-(100) surface with the water oxygen atom bound to the Ti^{4+} site with the two water hydrogen atoms lying approximately in the same plane above the $SrTiO_3$(100) surface. As there are no bridging oxygen atoms available for hydrogen bonding on the TiO_2-terminated surface to this water as there are on the TiO_2(110) surface, the protons of the water molecules interact with the surface ($R(H_{water}-O_{surf})$ = 2.23, 2.59 Å) through nonspecific electrostatic and dipolar interactions in agreement with the TPD data.[38] In the case of methanol adsorption onto TiO_2-terminated $SrTiO_3$(100), three surface oxygen-adsorbate proton interactions are available: one proton from the −OH group (in a manner similar to the water proton interaction) and two others arising from the $-CH_3$ group. These latter two protons lie approximately on the same plane above the $SrTiO_3$-(100) surface ($R(O_{surf}-H_{methyl\ group})$ = 2.81, 2.87 Å), enhancing the attractive interaction between the surface and the adsorbates. These interactions are reflected in the Mulliken population analyses as the hydrogen atomic charges change from +0.226 and +0.191 for the free methanol molecule to +0.259 and +0.243 for the adsorbed case. These additional proton−surface interactions for CH_3OH adsorption could lead to the increased binding energy compared to similar interactions of water on the same surface. In comparison, both water and methanol

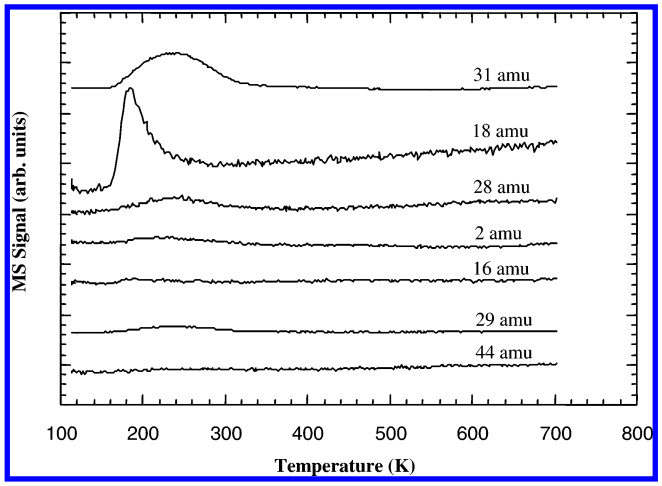

Figure 6. TPD spectra monitoring 2, 16, 18, 28, 29, 31, and 44 amu following adsorption of 1 langmuir of methanol on the stoichiometric TiO_2-terminated $SrTiO_3$(100) surfaces at 120 K.

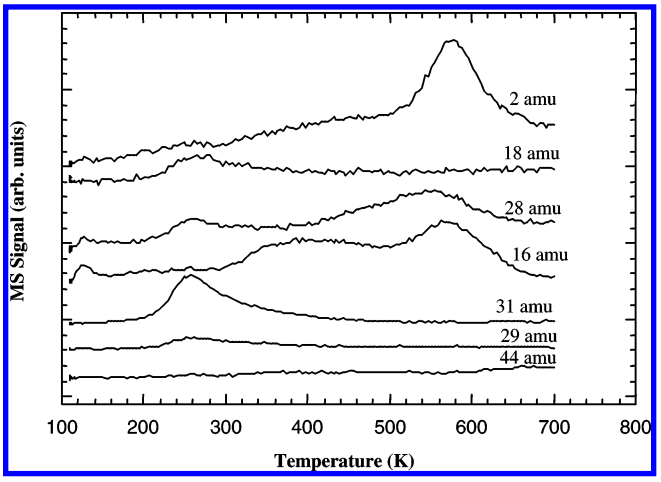

Figure 7. TPD spectra monitoring 2, 16, 18, 28, 29, 31, and 44 amu following adsorption of 1 langmuir of methanol on the reduced $SrTiO_3$-(100) surfaces at 120 K.

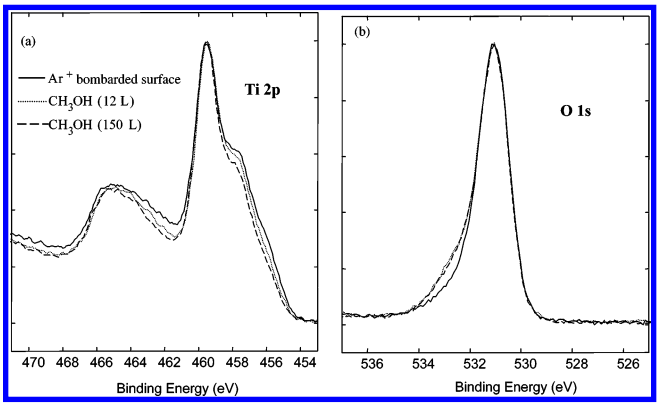

Figure 8. Ti 2p and O1s XPS spectra for a sputter-reduced $SrTiO_3$-(100) surface before and after exposures to methanol at 12 and 150 langmuirs at 300 K.

binding energies are greater than the 14.4 kcal/mol value for acetaldehyde[43] on the same surface. This would suggest that the oxygen hybridization, sp^3 as opposed to sp^2, is another factor affecting the binding nature of the adsorbate. Water and methanol being stronger bases than acetaldehyde produce stronger interactions with the stoichiometric strontium titanate surface.

Figure 6 displays TPD spectra monitoring 2 (H_2), 28 (CO), 18 (H_2O), 16 (CH_4), 29 (HCHO), 44 (CO_2), and 31 amu (CH_3OH) upon adsorption of 1 langmuir of methanol on the TiO_2-terminated stoichiometric $SrTiO_3$(100) surfaces at 120 K. For methanol on a stoichiometric $SrTiO_3$(100) surface, no desorption products are observed at temperatures above 350 K, indicating that methanol does not decompose on the TiO_2-terminated $SrTiO_3$(100) surface when adsorbed at 120 K. At temperatures lower than 300 K, methanol desorbs molecularly from this surface as observed in Figure 6. The small water TPD peak shown in Figure 6 is related to the desorption of the background water in the system. The same desorption feature for water is observed for a blank TPD run (without dosing methanol). The absence of decomposition products in TPD spectra taken upon methanol exposure at 120 K has also been reported previously on the TiO_2(110) surface.[5] However, TPD spectra taken at 300 K show a small fraction (about 15%) of methanol converted to HCHO and CH_3OH at high temperature (630 K) on the TiO_2-(110) surface.[2] The higher temperature of 300 K for CH_3OH exposure onto the TiO_2(110) surface may be responsible for the increased reactivity of methanol on this surface. Furthermore, decomposition products including CH_4, CH_2O, CO, and $(CH_3)_2O$ have been observed for methanol on TiO_2(100) surfaces.[7,8] The enhanced reactivity for methanol decomposition on the TiO_2-(100) surfaces is presumably induced by the variety of reactive surface sites on faceted TiO_2(100) surfaces.

Different TPD states are associated with either distinctive adsorption sites, phases, or the adsorbed state of molecules although TPD cannot be used to definitely identify the chemical state of adsorbates on surfaces. Since an ideal TiO_2-terminated $SrTiO_3$(100) surface has only one type of cation adsorption site (Figure 1) and LEED gave no indication of a two-dimensional phase change, the possibility of having a wide distribution of sites is unlikely on the TiO_2-terminated $SrTiO_3$(100) surface. Detailed microscopy studies using atomic force microscopy (AFM) or other techniques are required, however, to accurately determine the site distribution on theses surfaces.

4.2. Reactions on the Reduced $SrTiO_3$(100) Surfaces. Figure 7 displays the TPD spectra for desorption of CH_3OH from the reduced $SrTiO_3$(100). The TPD results indicate a significant difference in reactivity of CH_3OH on the stoichiometric (Figure 6) and on the reduced $SrTiO_3$(100) surfaces (Figure 7). A large amount of H_2 desorbs at 580 K during the TPD process following adsorption of CH_3OH on the reduced surface. Similar results are not found for adsorption of CH_3OH onto the stoichiometric surfaces. Broad desorption features for CO and CH_4 at temperatures above 300 K are also observed in the TPD spectra taken on the reduced surface. These results clearly indicate that defects on the reduced $SrTiO_3$(100) enhances the surface reactivity.

Figure 8 shows Ti 2p and O 1s XPS spectra taken at 300 K before and after CH_3OH exposure to a reduced $SrTiO_3$(100) surface. The spectrum for the reduced surface shows a large broadening in the Ti 2p peak at lower binding energy (BE) as well as a broadening in the O 1s peak at higher BE due to the presence of reduced Ti cations (approximately 30% Ti^{3+} and 20% Ti^{2+}) associated with the oxygen vacancies on the surface. XPS spectra of Sr 3d (not displayed here) show no change in the oxidation state of Sr and a small increase in the Sr-to-Ti ratio after Ar^+ bombardment. A slight narrowing in the Ti 2p peak at lower BE and a slight broadening of O 1s at higher BE are observed for the Ar^+-bombarded surface after CH_3OH exposures, indicating that a small number of reduced Ti cations are reoxidized by CH_3OH. Thus, the surface redox reaction coexists with the dissociation and decomposition reaction of the CH_3OH on the reduced $SrTiO_3$(100) surface. A slight broadening in the O 1s peak at higher BE is most likely due to

the formation of hydroxyl groups on the surface as a result of dissociative adsorption of CH_3OH, in agreement with our TPD data. Our previous XPS studies of methanol on reduced TiO_2-(100) and -(110) surfaces also show partial removal of defects upon saturation exposure of CH_3OH.[4]

The TPD spectra in Figure 7 indicate desorption of methane (CH_4, 16 amu), carbon monoxide (CO, 28 amu), and hydrogen (H_2, 2 amu) in the temperature range of 400−700 K, following adsorption of methanol on sputter-reduced $SrTiO_3$(100). The previous TPD studies of methanol on sputter-reduced TiO_2(001) surfaces showed desorption of decomposition products including CH_4 and CO, and CH_3OH above 500 K.[8] Methane is the only reaction product observed following exposure of methanol to an electron-irradiated (reduced) TiO_2(110) surface, and the amount of methane increases with the number of oxygen vacancy defects on the surface.[2] Methane was also observed at temperatures above 500 K for the reaction of CH_3OH on $SrTiO_3$ powder.[44] A previous study[8] of methanol on three characteristic (001) TiO_2 surfaces, the Ar^+-sputtered, the (011)-facetted, and the (114)-facetted surfaces, has found that the reactivity and selectivity largely depend on the surface structures and composition. Different main reaction pathways were proposed for CH_3OH on these different surfaces. The previously observed desorption products, such as dimethyl ether from the (114)-facetted surface and HCHO from the (110)-facetted TiO_2(001) surface, are not produced following adsorption of CH_3OH on the reduced $SrTiO_3$(100) surfaces. On the basis of our TPD and XPS data, the adsorption and decomposition of methanol on the reduced $SrTiO_3$(100) surface can be described as follows.

A small amount of dissociatively adsorbed CH_3OH on the reduced $SrTiO_3$(100) surface produced methoxide species on the surface, shown in eq 1, where "ad" and "l" stand for "adsorbed" and "lattice", respectively.

$$CH_3OH(ad) + O(l) \rightarrow CH_3O(ad) + OH(ad) \quad (1)$$

The coordinatively unsaturated Ti cations and adjacent oxygen anions on the reduced $SrTiO_3$(100) surface are responsible for the dissociative adsorption of CH_3OH on this surface.[8] The adsorbed methoxide species then recombine with surface OH groups to form CH_3OH desorbing from the reduced surface, resulting in a high-temperature tail extending up to 400 K in the TPD spectrum of methanol (Figure 7):

$$CH_3O(ad) + OH(ad) \rightarrow CH_3OH(g) + O(l) \quad (2)$$

where "g" is for gas phase. TPD spectra in Figure 7 display two broad peaks at 400 and 580 K for desorption of CH_4 from this surface. The higher temperature desorption state of CH_4 likely results from the following reactions proposed in a previous study of CH_3OH on (001)-facetted TiO_2 surfaces,[8]

$$CH_3O(ad) \rightarrow CH_3(ad) + O(l) \quad (3)$$

$$CH_3(ad) + H(ad) \rightarrow CH_4(ad) \quad (4)$$

The CH_3(ad) species produced in eq 3 may undergo further decomposition to produce adsorbed carbon and hydrogen atoms:

$$CH_3(ad) \rightarrow C(ad) + 3H(ad) \quad (5)$$

Another possible mechanism[2] to produce CH_4 through formation of methoxy on oxygen vacancy defects is

$$CH_3O(ad) + H(ad) \rightarrow CH_4(g) + O(l) \quad (6)$$

As opposed to the results obtained in the previous study of CH_3OH on TiO_2(001) surfaces,[8] recombination of adsorbed methoxy species with the adsorbed hydroxyl groups (eq 2) to produce methanol at higher temperature is not observed for CH_3OH on $SrTiO_3$(100) surfaces. The adsorbed hydrogen atoms on the reduced $SrTiO_3$(100) surface recombine at higher temperatures to produce H_2:

$$H(ad) + H(ad) \rightarrow H_2(g) \quad (7)$$

The adsorbed C and O atoms recombine at higher temperatures as well to produce CO:

$$C(ad) + O(l) \rightarrow CO(g) \quad (8)$$

Since the XPS results indicate reoxidation of reduced Ti cations upon adsorption of methanol on $SrTiO_3$(100), we propose a second reaction pathway for production of CH_4 at 400 K:

$$CH_3OH(ad) + 2Ti^{3+}(ad) \rightarrow CH_4(g) + 2Ti^{4+}(ad) + O^{2-}(ad) \quad (9)$$

Although the stoichiometric $SrTiO_3$(100) surface is inert to the decomposition of CH_3OH, the reduced surface is very reactive. The unsaturated Ti cations including reduced Ti states associated with the oxygen vacancies are responsible for the increased reactivity of the $SrTiO_3$ surfaces.

5. Conclusions

Interactions of methanol on stoichiometric and defective $SrTiO_3$(100) surfaces have been studied using temperature-programmed desorption (TPD), X-ray photoelectron spectroscopy (XPS), and first-principles density-functional calculations. Methanol was found to adsorb mostly nondissociatively on stoichiometric $SrTiO_3$(100) surfaces. Theoretical calculations show that methanol has weak adsorptive interactions with TiO_2-terminated $SrTiO_3$(100) surfaces, in agreement with the experimental results. The stronger binding of methanol on the TiO_2(110) surface than on $SrTiO_3$(100) surfaces is attributed to the more covalent nature of the Ti^{4+} cation sites and the unique surface structure due to the absence of the bridging oxygen atoms on the TiO_2-terminated $SrTiO_3$(100). As compared with the stoichiometric $SrTiO_3$(100) surfaces, the reduced $SrTiO_3$(100) surfaces exhibit higher reactivity. Adsorption of CH_3OH on the reduced $SrTiO_3$(100) surface produces the decomposition products of H_2, CO, and CH_4. The reduced Ti^{3+} cations are partially reoxidized by extraction of the adsorbed O atoms produced by the dissociation of adsorbed methanol.

Acknowledgment. This work has been supported by the Division of Materials Sciences Office of Basic Energy Sciences, U.S. Department of Energy (USDOE), and conducted at Environmental Molecular Science Laboratories (EMSL). Pacific Northwest National Laboratory is a multiprogram national laboratory operated for the USDOE by Battelle Memorial Institute under Contract DE-AC06-76RLO 1830.

References and Notes

(1) Azad, S.; Wang, L.-Q.; Szanyi, J.; Peden, C. H. F. *J. Vac. Sci. Technol., A* **2003**, *21*, 1307.
(2) Farfan-Arribas, E.; Madix, R. *J. Surf. Sci.* **2003**, *544*, 241.
(3) Onishi, H.; Aruga, T.; Egawa, C.; Iwasawa, Y. *Surf. Sci.* **1998**, *193*, 33.
(4) Wang, L. Q.; Ferris, K. F.; Winokur, J. P.; Shultz, A. N.; Baer, D. R.; Engelhard, M. H. *J. Vac. Sci. Technol., A* **1998**, *16*, 3034.
(5) Henderson, M. A.; Otero-Tapia, S.; Castro, M. E. *Faraday Discuss.* **1999**, *114*, 313.

(6) Henderson, M. A.; Otero-Tapia, S.; Castro, M. E. *Surf. Sci.* **1998**, *412/413*, 252.
(7) Roman, E.; Bustillo, F. J.; de Segovia, J. L. *Vacuum* **1990**, *41*, 40.
(8) Kim, K. S.; Barteau, M. A. *Surf. Sci.* **1989**, *223*, 13.
(9) Tero, R.; Fukui, K.-I.; Iwasawa, Y. *J. Phys. Chem. B* **2003**, *107*, 3207.
(10) Wrighton, M. S.; Ellis, A. B.; Wolczanski, P. T.; Morse, D. L.; Abrahamson, H. B.; Ginley, D. S. *J. Am. Chem. Soc.* **1976**, *98*, 2774.
(11) Yoshikawa, T.; Bowker, M. *Phys. Chem Chem. Phys.* **1999**, *1*, 913.
(12) Ferris, K. F.; Wang, L.-Q. *J. Vac. Sci. Technol., A* **1998**, *16*, 956.
(13) Goniakowski, J.; Gillan, M. J. *Surf. Sci.* **1996**, *350*, 145.
(14) Bredow, T.; Jug, K. *Surf. Sci.* **1995**, *327*, 398.
(15) Fahmi, A.; Minot, C. *Surf. Sci.* **1994**, *304*, 343.
(16) *Cerius2*, Version 4.0; Accelrys Inc.: San Diego, CA, 2000.
(17) Perdew, J. P.; Chevary, J. A.; Vosko, S. H.; Jackson, K. A.; Pederson, M. R.; Singh, D. J.; Fiolhais, C. *Phys. Rev. B* **1992**, *46*, 6671.
(18) Vanderbilt, D. *Phys. Rev. B* **1985**, *41*, 7892.
(19) *CASTEP*, Version 4.2.1; Accelrys Inc.: San Diego, CA, 2000. Milman, V.; Winkler, B.; White, J. A.; Pickard, C. J.; Payne, M. C.; Akhmatskaya, E. V.; and Nobes, R. H. *Int. J. Quantum Chem.* **2000**, *77*, 895.
(20) Hirshfeld, T. *Theor. Chim. Acta B* **1977**, *44*, 129.
(21) Delley, B. J. *Chem. Phys.* **2000**, *113*, 7756.
(22) Rodriguez, J. A.; Hanson, J. C.; Chaturvedi, S.; Maiti, A.; Brito, J. L. *J. Chem. Phys.* **2000**, *112*, 935.
(23) Rodriguez, J. A.; Maiti, A. J. *Phys. Chem B* **2000**, *104*, 3630.
(24) Castell, M. R. *Surf. Sci.* **2002**, *516*, 33.
(25) Jiang Q. D.; Zegenhagen, J. *Surf. Sci.* **1999**, *425*, 343.
(26) Jiang Q. D.; Zegenhagen, J. *Surf. Sci.* **1996**, *367*, L42.
(27) Tanaka, H.; Matsumoto, T.; Kawai, T.; Kawai, S. *Surf. Sci.* **1994**, *318*, 29.
(28) Matsumoto, T.; Tanaka, H.; Kawai, T.; Kawai, S. *Surf. Sci.* **1992**, *278*, L153.
(29) Kubo T.; Nozoye, H. *Phys. Rev. Lett.* **2001**, *86*, 1801.
(30) Andersen, J. E. T.; Moller P. *J. Appl. Phys. Lett.* **1990**, *56*, 1847.
(31) Naito, M.; Sato, H. *Physica C* **1994**, *229*, 1.
(32) Yoshimoto, M.; Maeda, T.; Shimozono, K.; Koinuma, H.; Shinohara, M.; Ishiyama, O.; Ohtani, F. *Appl. Phys. Lett.* **1994**, *65*, 3197.
(33) Nishimura, T.; Ikeda, A.; Namba, H.; Morishita, T.; Kida, Y. *Surf. Sci.* **1999**, *421*, 273.
(34) Thiel, P. A.; Madey, T. E. *Surf. Sci. Rep.* **1987**, *7*, 211.
(35) Henderson, M. A. *Surf. Sci.* **1994**, *319*, 315.
(36) Henderson, M. A. *Surf. Sci.* **1996**, *355*, 151.
(37) Henderson, M. A. *Langmuir* **1996**, *12*, 5093.
(38) Wang, L. Q.; Ferris, K. F.; Herman, G. S. *J. Vac. Sci. Technol., A* **2002**, *16*, 239.
(39) Stirniman, M. J.; Huang, C.; Smith, R. S.; Joyce, S. A.; Kay, B. D. *J. Chem. Phys.* **1996**, *105*, 1295.
(40) Rodriguez, J. A.; Azad, S.; Wang, L. Q.; Carcia, J.; Etxeberria, A.; Gonzalez, L. *J. Chem. Phys.* **2003**, *118*, 6562.
(41) Barr, T. L. *J. Vac. Sci. Technol., A* **1991**, *9*, 1793.
(42) Redhead, P. A. *Vacuum* **1962**, *12*, 203.
(43) Wang, L.-Q.; Ferris, K. F.; Azad, S.; Engelhard, M. H.; Peden, C. H. F. *J. Phys. Chem. B* **2004**, *108*, 1646.
(44) Aas, N.; Pringle, T. J.; Bowker, M. *J. Chem. Soc., Faraday Trans.* **1994**, *90*, 1015.